



# Design and Development of Engine Driven *Warqe (Ensete Ventricosum)* Decorticating Machine

Merga Workesa<sup>1,\*</sup>, Girma Gebresenbet<sup>2</sup>, Abebe Fanta<sup>3</sup>, Ashenafi Chaka<sup>4</sup>

<sup>1</sup>Bako Agricultural Engineering Research Center, Oromia Agricultural Research Institute, Addis Ababa, Ethiopia

<sup>2</sup>Department of Energy and Technology, Swedish University of Agricultural Sciences, Uppsala, Sweden

<sup>3</sup>Department of Agricultural Engineering, Haramaya University, Dire Dawa, Ethiopia

<sup>4</sup>Department of Horticulture, School of Agriculture, Ambo University, Ambo, Ethiopia

## Email address:

mergaw180@gmail.com (M. Workesa), Girma.Gebresenbet@slu.se (G. Gebresenbet), fantaalemitu@gmail.com (A. Fanta),

ashenafichaka@gmail.com (A. Chaka)

\*Corresponding author

## To cite this article:

Merga Workesa, Girma Gebresenbet, Abebe Fanta, Ashenafi Chaka. Design and Development of Engine Driven *Warqe (Ensete Ventricosum)* Decorticating Machine. *American Journal of Mechanical and Industrial Engineering*. Vol. 6, No. 2, 2021, pp. 17-27.

doi: 10.11648/j.ajmie.20210602.11

**Received:** April 4, 2021; **Accepted:** April 2, 2021; **Published:** June 22, 2021

---

**Abstract:** Warqe processing is carried out dominantly by women using traditional tools such as a bamboo scraper and wooden plank. The processing practice of warqe into food remained traditional and inefficient. The decortication process through which the separation of fiber and core takes place has been time consuming, much energy demanding and cause drudgery, and unhygienic due to the use of traditional decorticator that consisting of bamboo scraper and wooden plank. In light of the above, effort was made to develop mechanical warqe decorticator in order to improve the processing performances. The objective of this work was to design, fabricate the essential components, assemble, test and evaluate the performance in terms of decortication efficiency, throughput capacity, reliability, simplicity, safety, and cost. The functional parts of the machine included drum beater, breastplate, reduction gears, diesel engine, collecting box, chain and sprocket, feeding table, pulleys, transmission belts, rollers, engine seat, and bearings. The machine was manufactured using locally available materials to minimize cost. The design can further be improved to have better decorticating efficiency and throughput and low cost through the use of materials like aluminum and plastics rather than stainless steel and there is also the possibility of improving on the design and fabrication in view simplifying for mass production which can also attract private manufacturers.

**Keywords:** Breastplate, Decorticating, Drum Beater, Feeding Table, Power Transmission, Prototype

---

## 1. Introduction

*Warqe (Ensete ventricosum)* belongs to the family Musaceae and the genus *Ensete*. *Warqe* looks like a large, thick, single-stemmed banana plant. Both *warqe* and banana have an underground corm, a bundle of leaf sheaths that form the pseudostem, and large leaves [6].

*Warqe* can grow to the height of 10 meters with a pseudostem up to one meter in diameter. The stem has three parts; the upper-most portion is the pseudostem, which is made of a system of tightly clasping leaf bases or leaf sheaths, the underground corm an enlarged lower portion of the stem and a short section of stem near the soil line,

between the pseudostem and corm, is the true botanical stem [6]. It is usually multiplied by vegetative means and grown as clones [19].

The area under *warqe* production in Ethiopia is estimated to be over 321,362.43 hectares [7]. The average yield of *kocho* (non-dehydrated fermented product from the mixture of decorticated pseudostem, pulverized stem, and corm) is superior in food and the yield is over 43 tons/ha [5].

The report of [3] indicated that *warqe* is a popular staple crop in the central and southern parts of the country and is used as a food in major cities in Ethiopia such as Addis Ababa, Awassa, Dilla, Adama, Jimma, Wolayita Sodo, Hosaena, Wolkite, Woliso, Ambo, Bonga and Arba Minch

and other town and cities in the country.

Decortication is the process through which mechanical separation of fiber and core takes place. The equipment used for decortication is called a decorticator. *Warqe* fiber is also cleaned using a decorticator. A small spreading machine is used to separate fibers from the stem of the plant. An effective decortication can make following the cleaning process simpler and can improve the fiber quality significantly. One of the requirements of a decorticator is that it should not adversely affect the mechanical properties of the fiber. Hence, the design of a decorticating machine and the choice of operational parameters should consider this requirement [10].

Usually, women hold the leaf sheaths secured against vertically inclined wooden plank at halfway of its length with their heels from sited position to prevent the leaf sheath from slipping down during scraping. The scraping process of the soft material results in the production of fibers as a byproduct. The upper half of the leaf sheath was then turned upside down, for further scraping [17]. Scraping from the sited position is very common in the country, though [18] had reported the relevance of scraping from a standing position in Wolayita (Southern Ethiopia). Whatsoever, the case may be, the traditional way of *warqe* processing results in a lot of physical drudgery and strain among women involved in processing the crop.

Several Agricultural Research institutions have tried to develop devices that would reduce the tedium and time needed to process *warqe*. Women use bamboo scrapers for decortication and cloth squeezers for *bulla* making. Yet, there is still a great demand to device ways and means to ease the processing practice of this crop and to reduce drudgery and time requirement. Therefore the objective of this paper was to, develop and introduce a decorticator that could separate the pulp from the leaf sheath. Hence, this study was initiated to design, develop, test and evaluate the performance of engine driven *warqe* decorticating machine that could be affordable by the end users and can decrease the labor requirement in decorticating *warqe* as well as add value to the product.

## 2. Materials and Methods

### 2.1. Design Requirements

The important design factors considered in this design were the function, maintenance, reliability, safety and cost [12]. During the design of the decorticating machine, the following machine specifications such as continuous operation, efficiency and local availability of fabrication materials and spare parts were considered.

### 2.2. Design of Decorticating Machine

A decorticating machine is expected to have a reasonable decorticating capacity, high efficiency and quality fiber as a byproduct, comfort to the operator and affordability to the end users. Accordingly, a decorticating machine should

consist of feeding table, breastplate, drum housing, rollers, frame, engine, engine seat, driving and driven assembly (pulleys and belt) and collecting pan.

#### 2.2.1. Power Transmission Design and Selection

In the design of belts and pulleys power transmission system Eqns. 2 to 8 were used. Restriction of choice of belt section was raised from the viewpoint of minimum pulley diameter. The minimum smaller pulley diameter of 120 mm was selected for which belt section A was sufficient to transmit power from an engine to drum beater. The cross-sectional area of the belt was calculated by summing area 1, 2 and 3 of the trapezoidal section shown in the (Figure 11) and was found  $8.4 \times 10^{-5} \text{ m}^2$ . From top width,  $b = 13 \text{ m}$ , thickness,  $t = 8 \text{ mm}$  and by calculation, the bottom width  $\chi = 8 \text{ mm}$ . The groove angle of the pulley was taken as  $34^\circ$  which is the average of the range. In most agricultural machinery, rubber belt is used as a means of power transmission; hence rubber belt with a density of  $1140 \text{ kg/m}^3$  was used in this design. Accordingly, the mass of the rubber belt per meter is estimated to be  $0.096 \text{ kg/m}$ . The velocity of belt passing over the follower pulley can be calculated using Eqn. (1) [8].

$$V = \frac{\pi d_1 N_1}{60} \left( 1 - \frac{S}{100} \right) \quad (1)$$

Since the active arc of contact is not known, the belt slip on the smaller pulley at the first instance was considered to be 2% and the velocity is estimated as  $9.23 \text{ m/s}$ . The tension in the tight side of a power transmission belt can be calculated using Eqn. (2) as suggested by [5],

$$T_1 = T_{\max} - T_C \quad (2)$$

The centrifugal tension of the belt ( $T_C$ ) is given by;

$$T_C = mv^2 \quad (3)$$

Hence, the centrifugal force was estimated using Eqn. (3) to be  $8.16 \text{ N}$ . The maximum tension in the belt is given as,

$$T_{\max} = \sigma A \quad (4)$$

The mass of the belt per unit length,

$$m = \rho A \quad (5)$$

$$A = \left( \frac{b - \chi}{2} \right) \times t + \chi \times t \quad (6)$$

Thus, the maximum tension in the belt was calculated as  $235.20 \text{ N}$  using Eqn. (4). Therefore, tension on the tight side of the belt was calculated as  $227.04 \text{ N}$  by using Eqn. (2). The coefficient of friction between pulleys and belt can be determined using Eqn. (7) [11].

$$\mu = 0.54 - \frac{0.7}{2.4 + V} \quad (7)$$

where:  $V$  = velocity of belt (m/s). Coefficient of friction between pulley and the belt was estimated to be 0.48,  $T_c$  and  $T_{\max}$  = the centrifugal and maximum tension of the belt (N);  $A$  = cross sectional area of a belt ( $\text{mm}^2$ );  $m$  = mass per unit length (kg/m) of a belt;  $v$  = speed of belt (m/s);  $b$  = top width of the belt (mm);  $\chi$  = bottom width of the belt (mm);  $d_1$  = diameter of driving pulley (mm),  $N_1$  = speed of the driving pulley (rpm);  $S$  = slip (%);  $\sigma$  = Maximum allowable stress of belt (MPa);  $t$  = thickness of the belt (mm);  $\rho$  = density of belt material (Rubber) ( $\text{kg/m}^3$ );  $T_1$  = belt tension in tight side (N);  $T_2$  = belt tension in slank side (N);  $\mu$  = coefficient of friction between belt and pulley;  $\alpha_1$  = angle of wrap for smaller pulley (rad)

### 2.2.2. Estimation of Belt Length

Length of belt required to transmit power shall be calculated using Eqns. (8 and 9) as given by [8],

$$L = 2C + 1.57(D_1 + D_2) + \frac{(D_2 - D_1)^2}{4C} \quad (8)$$

where:  $D_1$  and  $D_2$  = diameters of driving and driven pulleys (mm);  $C$  = center to center distance between smaller and larger pulleys (mm);  $L$  = belt length (mm)

The Centre distance ( $C$ ) between the two pulleys must not be less than twice the diameter of the larger pulley [13].

$$C = 2D_2 \quad (9)$$

Length of a belt was calculated using Eqns. (10 and 11) and found out to be 1,374.00 mm and the nearest belt length of 1372.00 mm A 54, was used in the design. The length of belt used with three driven pulleys of different diameters was selected on the basis of speed ratios. Wrap angle on the smaller pulley is determined using Eqn. (10) while that of the big pulley can be estimated using Eqn. (11) [2].

$$\alpha_1 = 180 - 2 \sin^{-1} \left( \frac{D_2 - D_1}{2C} \right) \quad (10)$$

The wrap angle of the belt on the large pulley on the drum beater can be calculated using Eqn. (13) [2].

$$\alpha_2 = 180 + 2 \sin^{-1} \left( \frac{D_2 - D_1}{2C} \right) \quad (11)$$

where:  $\alpha_1$  = angle of wrap on smaller pulley (degree);  $\alpha_2$  = angle of wrap on larger pulley (degree);

Equations 12 and 13 were used to estimate wrap angles on smaller and larger pulleys. The wrap angles of small and large pulleys were 173.80 and 192.40 degrees, respectively. Belt tension ratio for v-belt can be calculated using Eqn. (12) [2].

$$\frac{T_1 - mv^2}{T_2 - mv^2} = e^{\frac{\mu \alpha_1}{\sin \frac{\beta}{2}}} \quad (12)$$

Tension at the slack side was estimated to be 53.17 N by using Eqn. (12). According to [8] torque on a shaft can be calculated using Eqn. (13).

$$T = (T_1 - T_2) \times \frac{D_2}{2} \quad (13)$$

where:  $T_1$  = tight side tension of belt (N);  $T_2$  = slack side tension of belt (N);  $D_2$  = diameter of the largest driven pulley (m);  $\beta$  = belt wedge angle (degree)

Torque on a shaft was calculated using Eqn. (13) and determined to be 18.43 Nm.

### 2.2.3. Chain and Sprocket Selection

Pitch of the chain shall be calculated using Eqn. (14) (Gupta and Khurmi, 2005).

$$P = D \sin \frac{\theta}{2} \quad (14)$$

$$\theta = \frac{360^\circ}{T} \quad (15)$$

Pitch of the chain was calculated using Eqns. (14) estimated to be 14.00 mm.

The sprocket outside diameter ( $D_o$ ), for satisfactory operation, is given by Eqn. (16) [8].

$$D_o = D + 0.8d_1 \quad (16)$$

where:  $d_1$  = Diameter of the chain roller (mm).

The sprocket outside diameter ( $D_o$ ) was determined by using Eqn. (16) and its value is 116.80 mm. The velocity ratio (VR) of a chain drive is given by Eqn. (17), [2].

$$V_R = \frac{N_1}{N_2} = \frac{N_{t_2}}{N_{t_1}} \quad (17)$$

where:  $N_1$  = Speed of rotation of smaller sprocket (rpm);  $N_2$  = Speed of rotation of larger sprocket (rpm);  $N_{t_1}$  = Number of teeth on the smaller sprocket;  $N_{t_2}$  = Number of teeth on the larger sprocket;  $V_R$  = velocity ratio;

The velocity ratio of the chain drive was calculated using Eqn. (17) and found to be 1.71. The length of the chain ( $L$ ) shall be calculated using Eqn. (18) below [8].

$$L = K \times P \quad (18)$$

where:  $L$  = length of the chain (mm);  $K$  = numbers of links;  $P$  = pitch of the chain (mm)

The length of the chain ( $L$ ) was calculated using Eqn. (18). The minimum center distance between the smaller and larger sprockets should be 30 to 50 times the pitch [8]. Assuming the center distance; between smaller and bigger sprocket to be 30 times the pitch in order to accommodate initial sag in the chain. Therefore the corrected center distance was calculated to be 415 mm. The numbers of chain links were obtained by using Eqn. (19) estimated to be 79. Based on this, the length of the chain was estimated to be 1.11 m. The

number of chain links can be obtained using Eqn. (19) [8].

$$K = \frac{N_{t1} + N_{t2}}{2} + \frac{2C}{P} + \left[ \frac{N_{t2} - N_{t1}}{2\pi} \right] \times \frac{P}{C} \quad (19)$$

where:  $C$  = center distance between sprockets (mm);  $N_{t1}$  = Number of teeth on the smaller sprocket;  $N_{t2}$  = Number of teeth on the larger sprocket

#### 2.2.4. Gear Design and Selection

The maximum value of the bending stresses (the permissible working stress), at the critical section, is given by the Eqn. (20) [13].

$$\sigma_w = \frac{M \times y}{I} \quad (20)$$

$$\text{But } M = W_T \times h, \quad y = \frac{t}{2} \text{ and } I = \frac{b \times t^3}{12}$$

Where:  $M$  = Maximum bending moment at the critical section (N-m);  $W_T$  = Tangential load acting on the tooth (N);  $h$  = Length of the tooth (mm);  $y$  = Half the thickness of the tooth ( $t$ ) at critical section (mm);  $I$  = Moment of inertia about the center line of the tooth (mm<sup>4</sup>);  $b$  = Width of gear face (mm);

To achieve the desired speed ratios, the number of teeth on driving gear had been determined to be 18 with a pressure angle of 20°. Assuming the gear shall have a pressure angle of 20° and full depth involute system the value of  $y$  in terms of the number of teeth shall be expressed as follows [13].

$$y = 0.154 - \frac{0.912}{N_t} \quad (21)$$

The full depth involute system value of 'y' was determined by using Eqn. (24) and found to be 0.103. The module ( $m$ ) of the selected gear is  $\frac{D}{T} = \frac{105}{18} = 5.83$  mm the standard module is 6 mm. Circular pitch for the two meshing gears having teeth  $T_1$  and  $T_2$  and diameters of  $D_1$  and  $D_2$  respectively can be calculated pitch using Eqn. (22) [13].

$$P_c = \frac{\pi D_1}{N_{t1}} \quad (22)$$

The pitch for the two meshing gears having teeth  $T_1 = 18$  and  $T_2$  and diameters  $D_1 = 105$  mm and  $D_2$ , the circular pitch was calculated using Eqn. (25) and found to be 18 mm. The face width of gear varies between 2  $P_c$  to 3  $P_c$  for cast teeth. Therefore, considering the face width of the gear to be 2  $P_c$ , and calculated to be 36 mm. substituting the values of  $M$ ,  $y$  and  $I$  into Eqn. (23), the working stress can be determined using the equation below.

$$\sigma_w = \frac{6(W_T \times h)}{b t^2} \quad (23)$$

Gear permissible working stress was calculated by Eqn. (24). The values of the velocity factor ( $C_v$ ) for ordinary cut gears operating at velocities up to 12.5 m / s was determined by using Eqn. (25). Gear permissible working stress can be calculated using Eqn. (24) [13].

$$\sigma_w = \sigma_0 \times C_v \quad (24)$$

where:  $\sigma_0$  = Allowable static stress (MPa);  $C_v$  = Velocity factor;  $N_t$  = number of teeth on the gear;  $N_{t1}$  = number of teeth on the driving gear.

The values of the velocity factor ( $C_v$ ) for ordinary cut gears operating at velocities up to 12.5 m / s are given by Eqn. (25),

$$C_v = \frac{3}{3 + V} \quad (25)$$

where,  $V$  = Pitch line velocity in m/s

The rotational speed of the driving gear having 105 mm diameter and 18 teeth was determined to be 612.5 rpm. Therefore, the pitch line velocity was calculated at 3.37 m/s. putting the value into Eqn. (25) the velocity factor was computed to be 0.47. Taking the value of 70 MPa as allowable static stresses for cast iron of medium grade, the working stress of the gear was calculated and found to be 32.90 MPa. The tangential load of the gear shall be calculated using Eqn. (26).

$$\begin{aligned} W_T &= \sigma_w \times b \times p_c \times \frac{x^2}{6k} = \sigma_w \times b \times p_c \times y \\ &= \sigma_w \times b \times \pi m \times y \end{aligned} \quad (26)$$

Therefore, substituting values into Eqn. (26), the tangential load on the gear was determined and is 2298.00 N. To drive the gear a tangential load of 374.20 N was applied from the drum beater shaft to the rollers. This value was by far smaller than the tangential load carrying capacity of the gear (374.2N < 2298.34N). Hence, the design of the gear is considered to be safe.

#### 2.2.5. Drumbeater Shaft Design

For a solid shaft having little or no axial loading, the diameter of the shaft shall be calculated using the equation given by the American Society of Mechanical Engineering [4] as shown below.

$$d^3 = \frac{16}{\pi S_a} \sqrt{(C_b k_b M_b)^2 + (C_t k_t T)^2} \quad (27)$$

where:  $T$  = torsional moment of the shaft (Nm);  $d$  = diameter of the shaft (m);  $M_b$  = bending moment (Nm);  $S_a$  = allowable stress (N/m<sup>2</sup>);  $C_b$  and  $C_t$  = Stress concentration factors due to bending and torsion respectively. Forces acting at each location of the shaft were computed separately and the vertical components of the forces are shown in Figure 1.

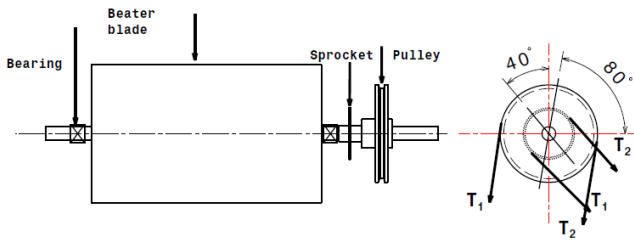


Figure 1. A layout of shaft components.

The net force of the V-belt pulley shall be computed using Eqn. (28) [15].

$$F_N = T_1 - T_2 \quad (28)$$

Substituting the values of  $T_1$  and  $T_2$  into Eqn. (28), the net driving force on the pulley was obtained as 173.73 N. The bending force due to net force was computed using Eqn. (29) and found out to be 260.81N. The bending force due to the net force is [15],

$$F_P = 1.5F_N \quad (29)$$

The bending force acts downward and inclined at an angle of  $80^\circ$  from the horizontal with respect to the pulley and downward inclined at an angle of  $40^\circ$  from the horizontal with respect to the sprocket wheel. The horizontal and vertical components of this net force are 45.29 N and 256.85 N, respectively. The bending force on the shaft carrying a sprocket wheel is equal to the tension in the tight side of the chain and calculated using Eqn. (30) [15].

$$F_S = \frac{2T}{D_s} \quad (30)$$

where:  $T$  = torsional moment of the shaft (Nm);  $D_s$  = diameter of sprocket (mm),

The bending force on the shaft carrying the sprocket wheel is equal to the tension in the tight side of the chain [15] and calculated by using Eqn. (29) found to be 335.09 N. The components of bending forces in the vertical and horizontal direction on sprocket wheel were calculated using equations below. Therefore, the bending forces in horizontal and vertical directions were determined to be 256.69 N and 215.39 N respectively. The components forces acting on the shaft and the reaction forces at the bearings are shown in Figure 2 below. So, the computation of the resultant bending moment was carried out by resolving the forces at the pulley, sprocket and reaction forces bearings.

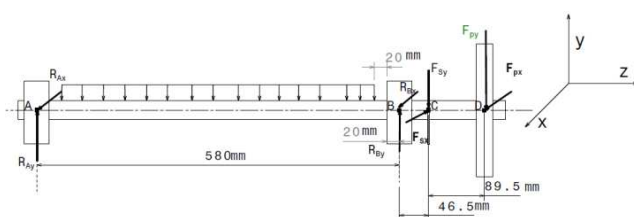


Figure 2. Free body diagram of on the shaft.

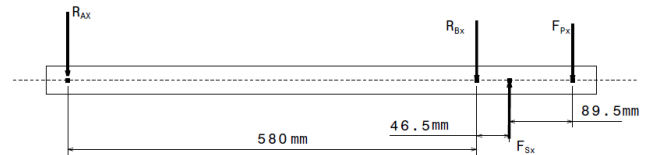


Figure 3. Free body diagram of forces on the horizontal plane.

where:  $R_{Ax}$  and  $R_{Bx}$  are reaction forces in the x-direction at bearings 'A' and 'B';  $F_{Sx}$  and  $F_{Px}$  resultant forces of the belt and the chain in the horizontal direction;

The values of the reaction forces were determined by taking the summation of a moment at preferable point. Therefore, the reaction force at bearing 'A' is 9.96 to the left and that at 'B' was determined to be 221.36 N. the reaction forces are shown in figure 4.

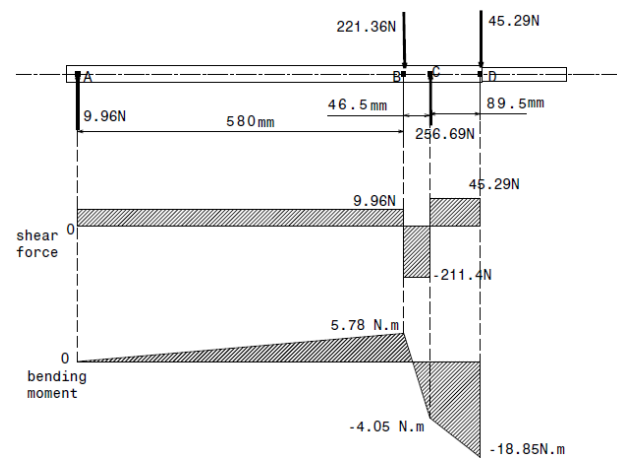


Figure 4. Shear force and bending moment diagram on the horizontal plane.

Similarly, the forces were resolved in the vertical direction in order to calculate reaction forces at bearings. The free body diagram of the shaft is shown in Figure 5.

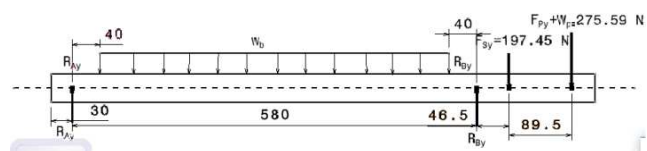


Figure 5. Free body diagram of reaction and resultant bending forces on a vertical plane.

The weight of beater blade was calculated by using volume and density and found out to be 105.95 N. Similarly, the weight of the three circular discs used to construct the beater drum was also estimated to 16.97 N. Neglecting the weight of the welds, the total load on the shaft was estimated to be 122.92 N which is the sum of the weight of the disk and the blade. The forces acting on the vertical plane are shown in Figure 6.

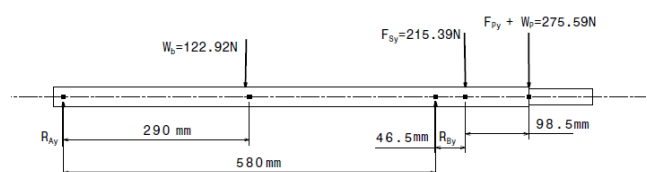


Figure 6. Free body diagram of forces on the vertical plane.

Reaction forces at bearings were determined and their values were  $R_{AY} = 13.71$  N (downwards) and  $R_{BY} = 608.87$  N (upwards). Using the computed value of the reaction and component forces, the magnitude of shear forces and bending moment diagram was drawn as shown in Figure 7.

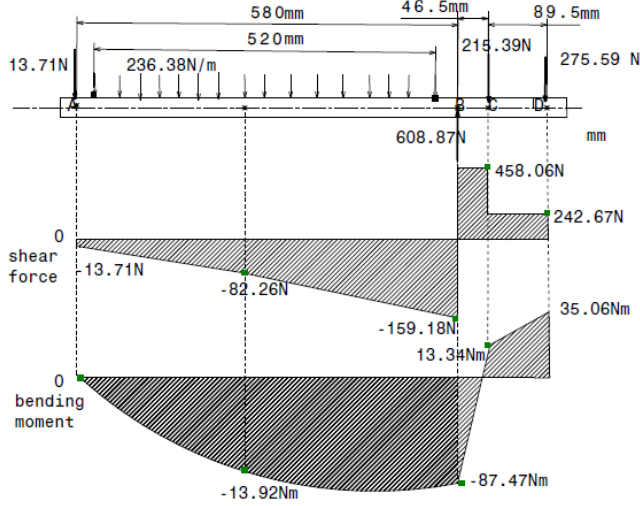


Figure 7. Shear force and bending moment diagram on a vertical plane.

The resultant maximum bending moment on the shaft was calculated using Eqn. (31).

$$M_b = \sqrt{M_v^2 + M_h^2} \quad (31)$$

The resultant bending moment with the highest value of 87.66 Nm was selected for design analysis.

A bearing catalog was used to determine the ratio of  $D/d$ ; was found to be between 1.20 and 1.50. The values of the constants ( $C_b$  and  $C_t$ ), used in Eqn. (27) are obtained as 2.15 for  $C_b$  and the value of  $C_t$  is 1.98 considered. As recommended by [13]  $K_b$  value of 1.20 and  $K_t$  value of 1.0 were used to estimate the minimum diameter of the shaft. The allowable shear stress ( $S_a$ ) of 40 MN/m<sup>2</sup> for a shaft with keyway was used. As a result, the minimum diameter of the shaft found to be 0.03 m (30mm). Since the calculated diameter of the shaft is within the standard shaft diameters, a 30 mm diameter stainless steel shaft was used in the construction of the decorticator.

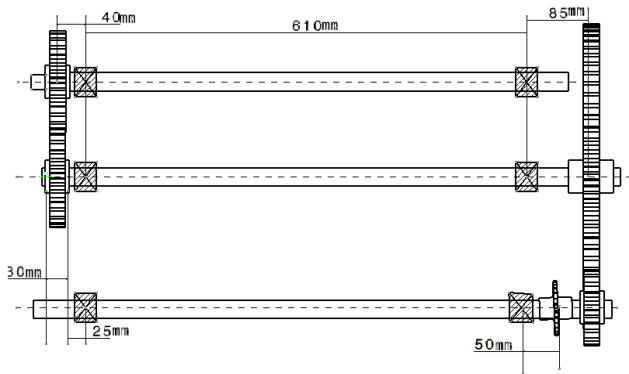


Figure 8. A layout of intermediate shaft and rollers.

## 2.2.6. Design of Power Transmitting Shaft to Rollers

Figure 8 shows the layout of and the components parts of power transmitting elements.

Figure 9 shows the details and arrangement of rollers power transmission. It is assumed that the total bending force on the shaft carrying the sprocket wheel is equal to the tension in the tight side of the chain. Assuming that the mass of smaller gear and sprocket wheel were negligible compared to the forces due to tension. The forces on the shaft were bending forces due to chain tension and; action and reaction forces of driving and driven gears. The tension on the tight side of the chain was determined to be 335.09 N and was equals to the bending force on the shaft.

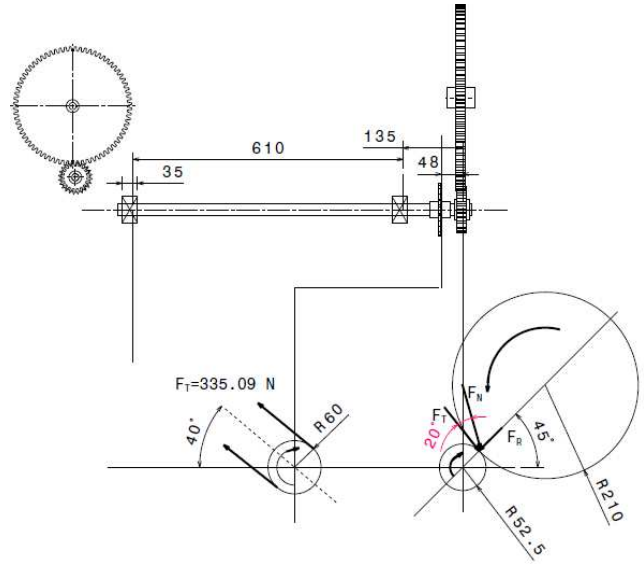


Figure 9. A layout of intermediate shaft (all dimensions in mm).

Resolve the tension force on the sprocket wheel into the horizontal and vertical components.

The horizontal component equals to:

$$F_{Sx} = F_T \cos \theta = 335.09 \text{ N} \times \cos 40^\circ = 256.69 \text{ N}$$

The vertical component equals to:

$$F_{Sy} = F_T \sin \theta = 335.09 \text{ N} \times \sin 40^\circ = 215.39 \text{ N}$$

The torque produced by the chain on the sprocket wheel was equal to the torque on the smaller gear. Therefore, the torque on the sprocket wheel was determined using Eqn. (30) and its value is 20.11 Nm. The tangential force on the gear was determined and its value was estimated to be 383.05 N. the radial force was computed directly from tangential force assuming pressure angle of 20° which is the most common one. The radial force, hence, is equal to 139.42 N.

Since the pinion gear meshed at 45° from the horizontal plane, the tangential and radial forces were resolved into vertical and horizontal planes. Therefore, force components due to tangential force in horizontal and vertical planes were computed to be 270.86 N and 270.86 and components forces due to radial force of the gear in horizontal and vertical



planes were 98.58 N and 98.58 N respectively. From the above-calculated values the resultant forces in the vertical and horizontal direction were determined by adding the forces acting in the same direction and subtracting forces acting in opposite directions in a given direction. Therefore, the total force in the horizontal direction on the pinion gear was determined as follow,

$$F_{Tx} = F_{tx} - F_{Rx} = 270.86 \text{ N} - 98.58 \text{ N} = 172.28 \text{ N}$$

The total force on the pinion in the vertical direction is given as follows,

$$F_{Ty} = F_{ty} + F_{Ry} = 270.86 \text{ N} + 98.58 \text{ N} = 369.44 \text{ N}$$

Forces shown in Figure 10 were used to determine reactions at bearings 'A' and 'B'.

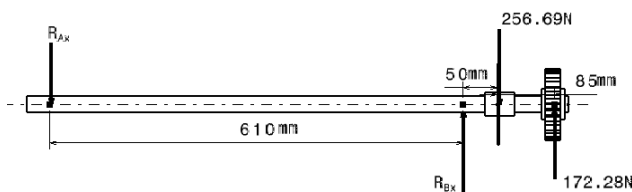


Figure 10. Free body diagram of the forces in the horizontal plane.

The shear force and bending moment diagram of the shaft in the horizontal plane is shown in Figure 11.

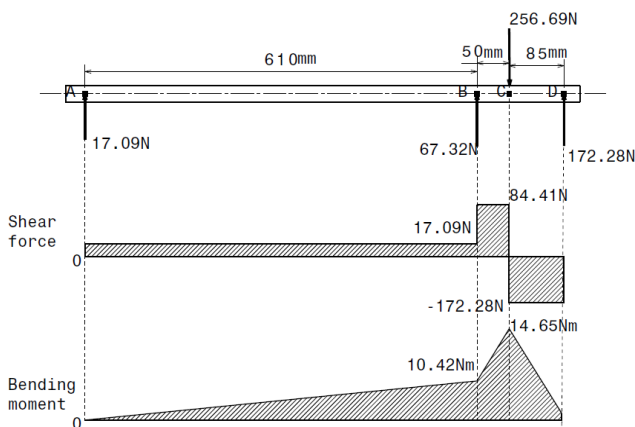


Figure 11. Shear force and bending moment diagram in the horizontal plane.

The free body diagrams of the forces in the vertical direction were shown in Figure 12. The reaction forces at bearings 'A' and 'B' were calculated based on the free body diagram.

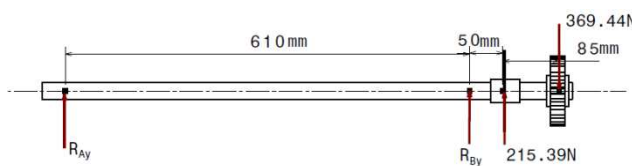


Figure 12. Free body diagram of forces in a vertical plane.

The loading, shear forces and bending moment on the shaft

are shown in Figure 13.

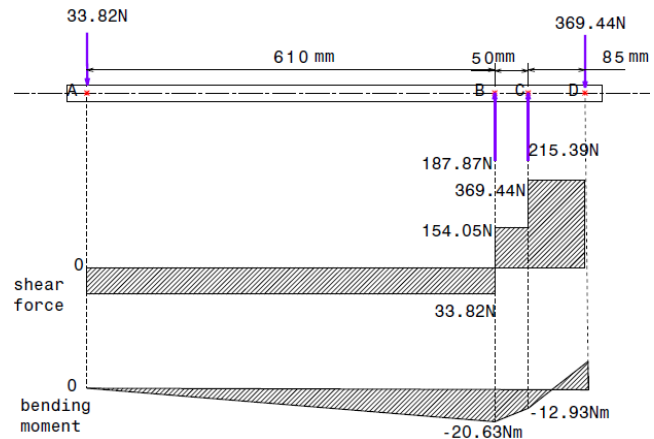


Figure 13. Shear force and bending moment diagram in the vertical plane.

The maximum bending moment on a shaft subjected both to horizontal and vertical forces were calculated using Eqn. (31).

$$M_b = \sqrt{M_v^2 + M_h^2} \quad (31)$$

As shown in figures 11 and 13 above the shaft was subjected bending moment in both horizontal and vertical at points B, C, and D. The maximum bending moment occurs at point 'B' which is 23.11 Nm. Eqn. (27) was used to determine the minimum diameter of the shaft; this diameter is 18.80 mm. The bore diameter of the selected for the pinion gear was 25 mm; hence, the shaft diameter to transmit power from drum beater to the rollers was decided to be 25 mm.

### 2.2.7. Design of Key

A key is a machinery component placed at the interface between a shaft and pulley/gear to make sure that the pulley/gear rotates with the shaft while transmitting power and motion. According to the maximum shear stress theory, the maximum shear stress on the shaft can be calculated using Eqn. (32) [14].

$$\tau_{\max} = \frac{S_y}{2F.S} \quad (32)$$

Maximum shear stress for the key was determined based on Eqn. (34). The yield strength of the selected material for key manufacturing is 352 MPa and a factor of safety of 3 was used. The maximum shear stress on the key can be determined based on Eqn. (33) [14].

$$\tau_k = \frac{S_{yk}}{2F.S} \quad (33)$$

The maximum shear stress in the key was estimated to be 58.67 MPa. The maximum torque transmitted by the shaft and key, determined by using Eqn. (34).

$$T = \frac{\pi \times \tau_{\max} \times d^3}{16} \quad (34)$$

where:  $T$  = shaft torque (Nm);  $d$  = shaft diameter (mm);  $S_y$  = yielding strength of the shaft ( $N/m^2$ );  $S_{yk}$  = yielding strength of the key ( $N/m^2$ ); F.S = factor of safety;

The key was designed to couple the pulley on the drum beater with that of drum beater shaft. The maximum torque transmitted calculated to be 319.25 Nm using Eqn. (34). The pulley was made of cast aluminum. Therefore, to be safe a square key with a width of 8 mm was used. Since the square key is equally strong in shearing and crushing. Failure of the key due to shearing occurs when,

$$T = \frac{L \times w \times \tau_k \times d}{2}$$

$$L = 0.045m = 45mm$$

By considering the failure of key due to crushing

$$T = L \times \frac{t}{2} \times \sigma_{ck} \times \frac{d}{2}$$

But  $\sigma_{ck} = \frac{S_{yk}}{F.S}$  therefore the length of the key should be calculated as follow,

$$L = 45mm$$

Therefore, the design of the key was safe for both for shear stress and crushing stress since the key length was equal.

### 2.2.8. Selection of Bearing

The selection of a bearing takes into consideration the load capacity and the geometry of the bearing ensuring that it can be installed conveniently in the machine. Design load of a bearing can be calculated using Eqn. (35) [20].

$$W = V \times R \quad (35)$$

where:  $W$  = load of the bearing (N);  $V$  = rotation factor 1.0 if the inner race of the bearing rotates and 1.2 if the outer race rotates;  $R$  = radial load (N)

The maximum radial load occurs on bearing at location 'B' where the resultant of the radial load at this bearing was calculated to be 50.33N. Therefore, the design load of the bearing was calculated using Eqn. (35). Assuming that the inner race of the bearing rotates,  $v = 1.0$ . Bearing load carrying capacity,  $P$ , is estimated using the Eqn. (36) [13].

$$P = \frac{W}{LD} \quad (36)$$

where:  $L$  = the length of bearing (m);  $D$  = the diameter of bearing (m)

Bearing number 206 with a bore of 30 mm and a width of 16 mm were selected since the minimum shaft diameter has been determined to be 30 mm. Hence, using Eqn. (36) the pressure on the bearing was determined to be  $104.85 \text{ KN/m}^2$ .

The design life of a bearing,  $L_d$ , can be estimated using Eqn. (37) [15].

$$L_d = \text{operation hour} \times \text{rotational speed} \quad (37)$$

Where,  $k = 3.00$  for ball bearings. The bearing number 206 load carrying the radial load of 128.15N and the shaft rotates at the highest speed of 1050 rpm; assume that the agricultural machine operation hour is 6000 hour. Therefore,

$$L_d = 6000h \times 1050 \text{ rpm} \times 60 \text{ min/h} = 3.78 \times 10^8 \text{ revolutions}$$

Basic dynamic load rating of a bearing can be calculated using Eqn. (38) below.

$$C = P_d \times \left( \frac{L_d}{10^6} \right)^{\frac{1}{k}} \quad (38)$$

where:  $k = 3.00$  for ball bearings and 3.33 for roller bearings;  $C$  = dynamic load of the bearing (N);  $P_d$  = design load of the bearing (N);  $L_d$  = design life of the bearing

Basic dynamic load rating of the bearing was calculated by Eqn. (38) and found to be 363.91 N. Since, the basic dynamic load rating of the bearing selected is by far less than the dynamic rating load given by manufacturers, that is 363.91N < 15,300N; the design is safe.

### 2.2.9. Design of Pulleys

Based on the required speed, the diameter of driving and the driven pulley was estimated using Eqn. (39) [1].

$$N_1 D_1 = N_2 D_2 \quad (40)$$

Since there were three levels of drum beater speed, the diameter of the driving pulley was 120 mm that of driven pulleys were determined from speed ratios were 212, 190 and 171mm.

The width of the pulley or face of the pulley ( $B$ ) is usually made 25% greater than the width of the belt ( $b$ ) and Eqn. (41) [14] can be used to estimate the width of the pulley.

$$B = b + 0.25b = 1.25b \quad (41)$$

The thickness ( $t$ ) of a pulley rim for a single belt can be calculated using Eqn. (42 or 43) [14].

$$t_1 = \frac{D}{300} + 2mm \quad (42)$$

$$t_2 = \frac{D}{200} + 3mm \quad (43)$$

where:  $N_1$  = maximum angular speed of driven pulley (rpm);  $N_2$  = maximum angular speed of driving pulley, (rpm);  $D_1$  = diameter of driven pulley (mm);  $B$  = width of pulley (mm);  $b$  = width of belt (mm);  $t_1$  = rim thickness of the driving pulley (mm);  $t_2$  = thickness of the driven pulley (mm);  $D_2$  = diameter of driving pulley (mm);  $D$  = can be used as diameter driving or driven pulley (mm). The computed thicknesses of the



pulley rim were almost similar for all; hence, the maximum thickness, i.e. 4.1 mm was selected. Assuming uniform rim thickness, the stress in the pulley can be calculated using Eqn. (44) [14].

$$\sigma_0 = \frac{\rho \times r_0^2 \times \omega^2 \times (3 + \nu)}{8g} \quad (44)$$

Pulleys are considered as a flywheel which is rotating the disk, centrifugal stresses act upon its distributed mass and attempt to pull it apart. Considering the rim thickness uniform, constant stress in the pulley was calculated based on Eqn. (43) and equal to 15.22 KPa. For constant thickness pulley rim, with a central hole, the radial and tangential stresses can be estimated by Eqn. (45) [14].

The radial stress on pulley rim: -

$$\sigma_r = \sigma_0 \times \left( 1 - \frac{r^2}{r_0^2} + \frac{r_i^2}{r_0^2} - \frac{r_i^2}{r^2} \right) \quad (45)$$

The tangential stress on pulley rim: -

$$\sigma_t = \sigma_0 \times \left( 1 - \left( \frac{1 + 3\nu}{3 + \nu} \right) \frac{r^2}{r_0^2} + \frac{r_i^2}{r_0^2} + \frac{r_i^2}{r^2} \right) \quad (46)$$

where:  $\sigma_0$  = constant stress (N/m<sup>2</sup>);  $\sigma_r$  = Radial stress of the rim (N/m<sup>2</sup>);  $\sigma_t$  = Tangential or bending stress of the rim (N/m<sup>2</sup>);  $r$  = mean radius of the rim (m);  $r_i$  = inner radius of the rim (m);  $r_0$  = outer radius of the rim (m);  $\rho$  = density of rim material (kg/m<sup>3</sup>);  $\omega$  = angular velocity of the flywheel (rad/s);  $\nu$  = poison's ratio.

The radial and tangential stresses of the pulley were computed to be 15.22 KPa and 35.20 KPa respectively considering the poison's ratio of aluminum cast 0.33. Therefore, the total stress in the rim was calculated to 50.42 KPa.

$$\sigma_{total} = \sigma_t + \sigma_r = 35.20 \text{ KPa} + 15.22 \text{ KPa} = 50.42 \text{ KPa}$$

Since the total stress in the rim was lower than the recommended stress, i.e. 15Mpa, the design is safe.

### 2.3. Constructions of the Prototype Machine Components

The fabrication of the prototype machine was accomplished on the basis of the design specification predetermined dimensions for each component. Design of the component parts of the decorticating machine was presented using solid work and CATIA software.

#### 2.3.1. Frame

The frame has a trapezoidal shape, 1000 mm by 600 mm at the base and 600 mm by 550 mm at the top, constructed from 40 mm by 40 mm by 4 mm angle iron. The standard minimum ratio of top and bottom lengths of a trapezoidal frame is given as  $L_1/L_2 = 0.5$  [9, 16]. The ratios of 0.60 and 0.92 were used for the base and top of the trapezoidal frame, respectively Figure 14.

Where:  $L_1$  and  $L_2$  = length of the frame at the top and the bottom (m), respectively

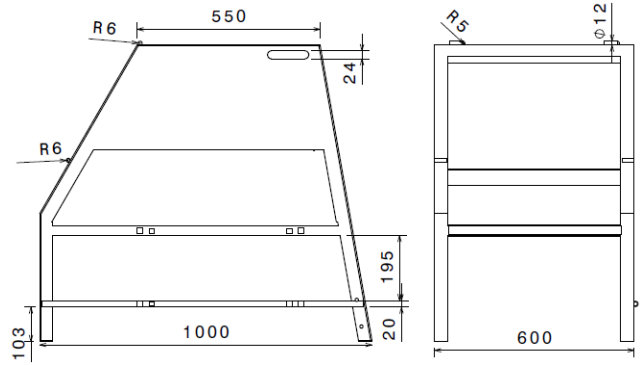


Figure 14. Views of the decorticating machine frame (A- Front view, B- Left view) (all dimensions are in mm).

#### 2.3.2. Beater Drum

The beater drum is a closed-ended rotating cylinder with blunt stainless steel welded on rolled circular disk stainless steel of 1.5 mm thickness. The beater drum consists of beater blades, end cover disk, and shaft. The cylinder was made by welding stainless steel flat between two disk plates with a length of 500 mm and intermediate disk were welded on the shaft (Figure 15).

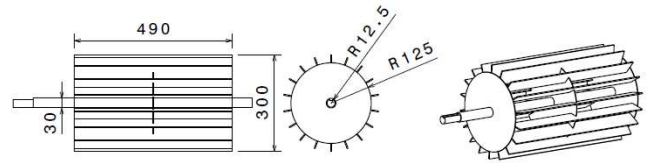


Figure 15. Views drum beater (A-right view, B-Front view, C-Isometric view) (all dimensions are in mm).

#### 2.3.3. Blades

Blades used in decorticating prototype machine were flat stainless steel of 500 mm by 50 mm by 3 mm with blunted edges and fixed on the drum at an angular spacing of 20°. The blunt edge avoids chopping the fiber. The numbers of blades ( $n$ ) were determined based on the decorticating quality using Eqns. (47) and (48).

$$n = \frac{2\pi}{\theta} \quad (47)$$

The number of blades calculated was 18 (eighteen) by assuming  $\theta$  to be 0.35 radian according to Eqn. (47). Considering the maximum drum speed level of 1050 rpm and pitch of 5 mm, the leaf sheath feeding speed into the machine was determined using Eqn.(48) below.

$$p = \frac{2\pi \times v}{\omega \times n} \quad (48)$$

$$v = \frac{p\omega n}{2\pi} = \frac{0.005 \times 1050 \times 18}{2 \times 3.14 \times 60} \text{ m/s} = 0.25 \text{ m/s}$$

where: P = pitch of the tissue extracted from the leaf sheath

(0.005m);  $v$  = linear feeding speed of the leaf sheath to the decorticator (0.25m/s);  $\omega$  = angular velocity of the drum beater (1050 rpm);  $n$  = number of blades on the cylinder (18);  $\theta$  = angle between two consecutive blades (20 degrees).

#### 2.3.4. Feeding Table

The feeding table was constructed from timber to protect metallic components from corroding and to minimize cost. The size of the feeding table was 580 mm by 350 mm by 40 mm Figure 16 and consisted of small horizontal rollers of 50 mm diameter to reduce frictional resistance between the feeding table and the leaf sheath.

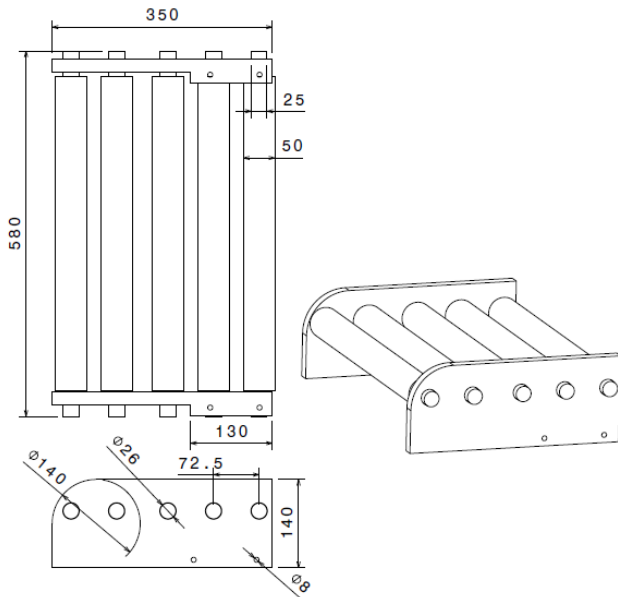


Figure 16. Views of rolling feeding table (all dimensions are in mm).

#### 2.3.5. Breastplate

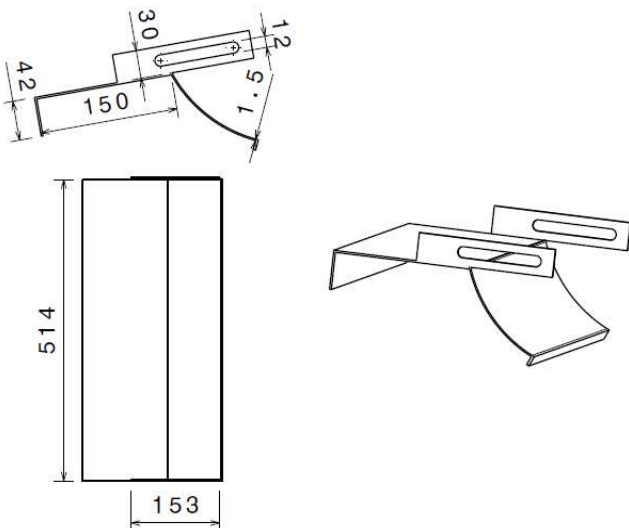


Figure 17. Views of breastplate (all dimensions are in mm).

The curved part of the breastplate has a curved length less than a quarter of the semi-circle and was made out of 1.50 mm thick rolled stainless steel sheet metal. The clearance

between drum beater and the breastplate was adjusted by sliding the breastplate back and forth and locking it at the desired position using slotted wings and bolts and nuts as shown in Figure 17.

#### 2.3.6. Collecting Box or Pan

The collecting pan is meant to collect decorticated pulp and squeezed juice during decortication. The collector was made out of plank with a thickness of 20 mm and coated with polyethylene plastic. The collecting pan has the shape and dimensions shown in Figure 18.

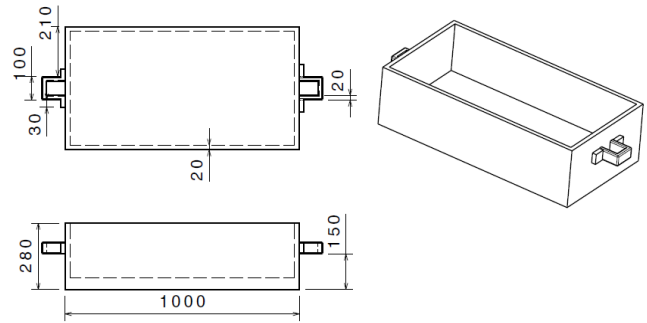


Figure 18. Views of collecting pan (all dimension in mm).

#### 2.3.7. Rollers

The main application of the rollers were to assist the feeding mechanism by gripping the leaf sheath and pushing it into the decortivating unit. It was used to maintain uniform feed rate into the decorticator. The rollers were made of 3 inches galvanized water pipe, diameter 25 mm and provided with mild steel shaft and pinion gears as power transmitting system.

#### 2.3.8. Transport Wheel

Transport wheels were manufactured by rolling mild steel sheet metal thickness of 6 mm and having spokes with a diameter of 12 mm; where the square hollow section was used to construct the axle capable carrying the entire weight of the machine Figure 19.

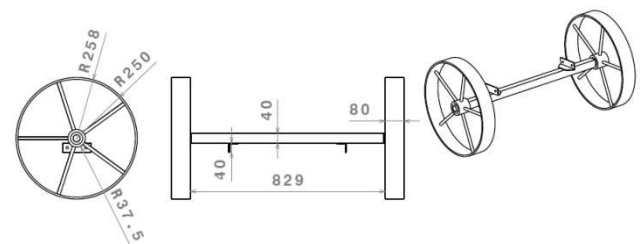


Figure 19. Transport wheel, (1-side view, 2-front view, 3-isometric view) (all dimensions are in mm).

## 3. Conclusion and recommendation

The design and construction of *warqe* decortivating machine have been carried out using available materials available on the local market. The machine weighs 110 kg consisting of wheels for transportation from one place to another. The improved traditional decortivating implement

had a capacity of decorticating one *warqe* plant in 3.36 hour but, using decorticating machine it only takes 0.20 hour to decorticate per plant. The design can still be improved to have more efficient *warqe* decortication at a relatively low cost by using manufacturing materials like aluminum and plastics other than stainless steel. It is recommended to look into the possibility of improving on the design and fabrication with a view of going into mass production which can also create a possibility for income generation.

## Acknowledgements

I acknowledge with great pleasure all the staff members of Bako Agricultural Engineering Research Center, who helped me during the manufacturing of the prototype and evaluating the performance of the machine, especially Ayele Haile Mariam, Getacho Buno and Kebede Sardo. Many my colleagues and friends whom I have known during my study period, here at Haramaya University, deserve my special thanks. I wish to place on record my deep sense of gratitude to the Oromia Agricultural Research Institute (OARI) and the German Federal Ministry of Education and Research for funding the RELOAD project at Ambo University.

## References

- [1] Aaron, D. 1975. Machine Design. In Theory and Practice. London, Collier Macmillan international.
- [2] Akintunde, B. O., Oyawale F. A. and Akintunde T. Y. 2005. Design and Fabrication of a Cassava Peeling Machine. *Nigerian Food Journal* 23, 231-238.
- [3] Ashanafi Chaka, Kenea Taddese and Girma Gebresenbet. 2016. Supply and Value Chain Analyses of Warqe Food Products in Relation to Post-harvest Losses, Swedish University Agricultural Sciences, Department of Energy and Technology, Uppsala.
- [4] ASME. 1995. Design of Transmission Shafting. American Society of Mechanical Engineering, New York, NY USA.
- [5] Atnafua and Endale. 2008. Food production and nutritional value of Enset. Proceedings of Enset National workshop, 9-14 August 2010, Wolkite, Ethiopia.
- [6] Brandt, S. A., Spring, A., Hiebsch C., McCabe J. T., Tabogie E., Diro, Wolde Michael, Yntiso G., Shigeta, M., and Tesfaye. (1997). Enset-based agricultural systems in Ethiopia. American Association for the Advancement of Science.
- [7] Ethiopian Central Statistical Agency (ECSA). 2013. Report on Area and Crop Production forecast for Major Crops Dec. 2013. Addis Ababa, Ethiopia.
- [8] Gupta, J. K., and Khurmi, R. S. 2005. A Textbook of Machine Design. S. I. Units. Eurasis Publishing House (PVT) Limited, New Delhi. pp. 16-52, 120-180, 509-557, 624-758 and 962-1020.
- [9] Hannah, J. and Stephens, R. C. 1984. 4th ed. *Mechanics of machine*. London, Edward Arnold.
- [10] Jinke, X. 2010. Analysis and design of Hemp Fiber decorticators, thesis, Department of Biosystems Engineering, University of Manitoba, Winnipeg.
- [11] Lingaiah, K. 2003. Machine Design Databook, second edition. McGraw-Hill Education: New York.
- [12] Norton, R. 2006. Design of Machinery. An Introduction to the Synthesis and Analysis of Mechanisms and Machines.
- [13] Richard, G. B., and Nisbett, J. K. (2006). Shigley's Mechanical Engineering Design, eighth edition, McGraw-Hill, New York, USA.
- [14] Richard, G. B., and Nisbett, J. K. (2011). Shigley's Mechanical Engineering Design, ninth edition, McGraw-Hill, New York, USA.
- [15] Robert, L. M. 2004. Machine Elements in Mechanical Design, Fourth Edition, Pearson Education Ltd.
- [16] Shigley, J. E. 1980. Engineering design 4th edition McGraw-Hill Coy, NY.
- [17] Tariku Hunduma, and Mogessie Ashenafi. 2011. 'Traditional Enset (*Ensete ventricosum*) processing techniques in Some Parts of West Shewa Zone, Ethiopia', 37-58.
- [18] Tedla and Abebe. 1994. Study of "Enset" processing and development of 'enset' processing tools in the southern regions of Ethiopia. ACA/NOR AGRIC Research Collaboration Project.
- [19] Tsegaye. 2002. Indigenous Production, Genetic Diversity and Crop Ecology of Enset (*Enset ventricosum* (Welw.) Cheesman). PhD Thesis, Wageningen University, Netherlands.